Available online at www.sciencedirect.com
ScienceDirect
Bioorganic & Medicinal Chemistry Letters
Bioorganic & Medicinal Chemistry Letters 17 (2007) 5671–5676

Kinesin spindle protein (KSP) inhibitors. Part 7: Design and synthesis of 3,3-disubstituted dihydropyrazolobenzoxazines as potent inhibitors of the mitotic kinesin KSP

Robert M. Garbaccio,[a,*] Edward S. Tasber,[a] Lou Anne Neilson,[a] Paul J. Coleman,[a] Mark E. Fraley,[a] Christy Olson,[a] Jeff Bergman,[a] Maricel Torrent,[a] Carolyn A. Buser,[b] Keith Rickert,[b] Eileen S. Walsh,[b] Kelly Hamilton,[b] Robert B. Lobell,[b] Weikang Tao,[b] Vicki J. South,[b] Ronald E. Diehl,[b] Joseph P. Davide,[b] Youwei Yan,[c] Lawrence C. Kuo,[c] Chunze Li,[d] Thomayant Prueksaritanont,[d] Carmen Fernandez-Metzler,[d] Elizabeth A. Mahan,[d] Donald E. Slaughter,[d] Joseph J. Salata,[e] Nancy E. Kohl,[d] Hans E. Huber[d] and George D. Hartman[a]

[a]*Department of Medicinal Chemistry, Merck Research Laboratories, West Point, PA 19486, USA*
[b]*Department of Cancer Research, Merck Research Laboratories, West Point, PA 19486, USA*
[c]*Department of Structural Biology, Merck Research Laboratories, West Point, PA 19486, USA*
[d]*Department of Drug Metabolism, Merck Research Laboratories, West Point, PA 19486, USA*
[e]*Department of Cellular Safety, Merck Research Laboratories, West Point, PA 19486, USA*

Received 30 May 2007; revised 17 July 2007; accepted 18 July 2007
Available online 21 August 2007

Abstract—Observations from two structurally related series of KSP inhibitors led to the proposal and discovery of dihydropyrazolobenzoxazines that possess ideal properties for cancer drug development. The synthesis and characterization of this class of inhibitors along with relevant pharmacokinetic and in vivo data are presented. The synthesis is highlighted by a key [3+2] cycloaddition to form the pyrazolobenzoxazine core followed by diastereospecific installation of a quaternary center.

In the preceding communication, the design, synthesis, and characterization of allosteric dihydropyrazole-based inhibitors of KSP (kinesin spindle protein) as novel anti-mitotics were described.[1] This effort resulted in the identification of water-soluble inhibitors (e.g., **1**, Fig. 1) that demonstrated pharmacokinetics suitable for iv administration and excellent in vivo potency. In addition, these compounds were designed to avoid Pgp-efflux, a potential mechanism for chemotherapeutic resistance in the clinic.

In parallel to these developments, a structurally related chromenopyrazole lead was identified by HTS and upon resolution of enantiomers afforded the (3*S*,3*aS*) *cis* enantiomer **2** as the active component (KSP IC_{50} = 800 nM) (Fig. 1). Due to the poor solubility displayed by the chromenopyrazole series, a novel series of dihydropyrazolobenzoxazines (e.g., **3**) was envisioned by simple rearrangement of the pyrazole nitrogens and incorporation of the 8-fluorine substitution that was found to enhance potency in prior efforts.[1] Upon synthesis, kinesin spindle protein inhibitor (KSPi) **3** was found to have good potency (KSP IC_{50} = 155 nM) and improved physical properties compared to **2**.

Drawing from reported advances in KSP inhibitor design within our group, we sought to incorporate the weakly basic amine tethered to the dihydropyrazole[2] (e.g., **1**) into these dihydropyrazolobenzoxazine cores (**3** → **4**) with the goal of improving potency and solubility while maintaining activity in a P-glycoprotein (Pgp) overexpressing cell line.

Keywords: KSP inhibitors; Anti-mitotics; Multidrug-resistance; Pgp; hERG; Kinesins; Pyrazolobenzoxazines; [3+2] Cycloaddition; Quaternary center; Kinesin spindle protein; Cancer.
* Corresponding author. Tel.: +1 215 652 5391; fax: +1 215 652 6345; e-mail: robert_garbaccio@merck.com

0960-894X/$ - see front matter © 2007 Elsevier Ltd. All rights reserved.
doi:10.1016/j.bmcl.2007.07.067

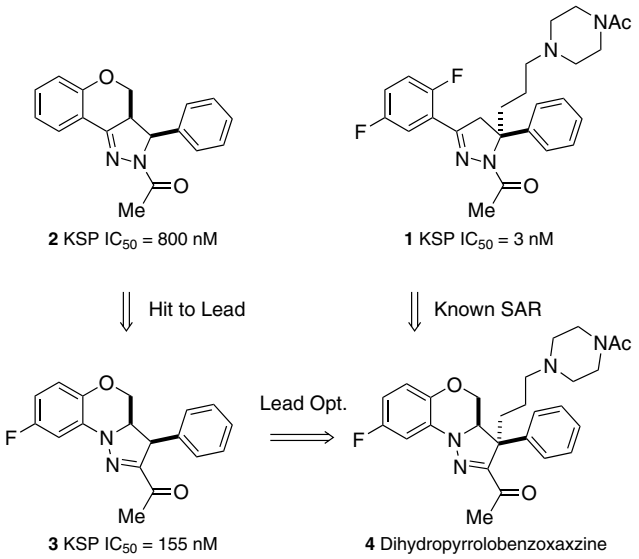

Figure 1. HTS hit **2**, lead **3** and related dihydropyrazole **1** that led to dihydropyrazolobenzoxazine proposal **4**.

A key observation made in the synthesis of the initial dihydropyrazolobenzoxazine **3** was a troublesome epimerization seen at C-4 under basic conditions. This observation suggested that formation of a quaternary center through anion chemistry would provide synthetic access to the proposed target. This report addresses the outcome of this proposal, and the full characterization of the KSP inhibitors produced in this effort.

The synthetic route[3] to the dihydropyrazolobenzoxazine tricycle initiated with alkylation of 4-fluoro-2-nitrophenol **5** with *trans*-3-cinnamyl chloride (**6**, Scheme 1) to give the corresponding ether **7** in excellent yield after recrystallization. The choice of the olefin geometry dictates the relative stereochemical outcome for C4/C5, but given the plans to deprotonate the C4 center, the decision to employ the *trans*-isomer was based on its commercial availability. Following efficient reduction of the nitro arene **7** by zinc metal, oxidation and conversion to the crystalline hydrazono-acetate **9** (Japp–Klingemann reaction) was accomplished with sodium-nitrite in the presence of ethyl 2-chloro-3-oxobutanoate in variable (65–92%) but good yield.

In the key [3+2] intramolecular cycloaddition of the cinnamyl olefin with an in-situ formed nitrile imine,[4] the major product (40% isolated yield) was found to be the benzoxadiazene (**12**, Scheme 2) that arises from an undesired competitive Claisen rearrangement of the cinnamyl ether onto the fluoroarene, followed by attack of the revealed phenol onto the chloroimine.[4] The desired *trans*-dihydropyrazolobenzoxazine **10** was isolated only in 35% yield under optimized conditions. This stands in contrast to the synthetic route that initiated with *cis*-3-cinnamyl chloride and provided the desired *cis*-tricycle **14** in a superior 65% yield without observation of this undesired reaction pathway (Scheme 3). Presumably, the *cis*-isomer cannot easily access the transition state required for the sigmatropic rearrangement. The conclusion from investigation of these two routes was that the extra two steps required for the synthesis of *cis*-cinnamyl chloride[5] result in a doubling of yield for the key [3+2] cycloaddition step. Both *trans*- and *cis*-esters (**10** and **14**) were directly transformed to the Weinreb amides (**11** and **15**) that would act as the alkylation substrate for stereospecific installation of the quaternary center.[6]

Alkylation at C4 of either *trans*-**11** or *cis*-**15** gave, as expected, the same result (Scheme 4). Deprotonation with LiHMDS occurred cleanly at −78 °C and reaction of the stabilized lithium anion with allyl bromide occurred with high *trans*-diastereospecificity (>20:1) to provide the quaternary center displayed in **16** in 69% isolated yield. These results are consistent with approach of the electrophile via the less-hindered face opposite to the methylene-oxy bridge. Elaboration of the olefin to the desired propyl amine and conversion of the Weinreb amide to the potent methyl ketone remained as the final synthetic hurdles. Hydroboration of the terminal olefin yielded the primary alcohol **17** that was then treated with methyllithium under optimized conditions. The desired methyl ketone **18** was isolated in 72% yield, and the major side product was found to be demethoxylation of the amide (15%) as has been reported elsewhere.[7] Oxidation of the primary alcohol to the aldehyde **19** with

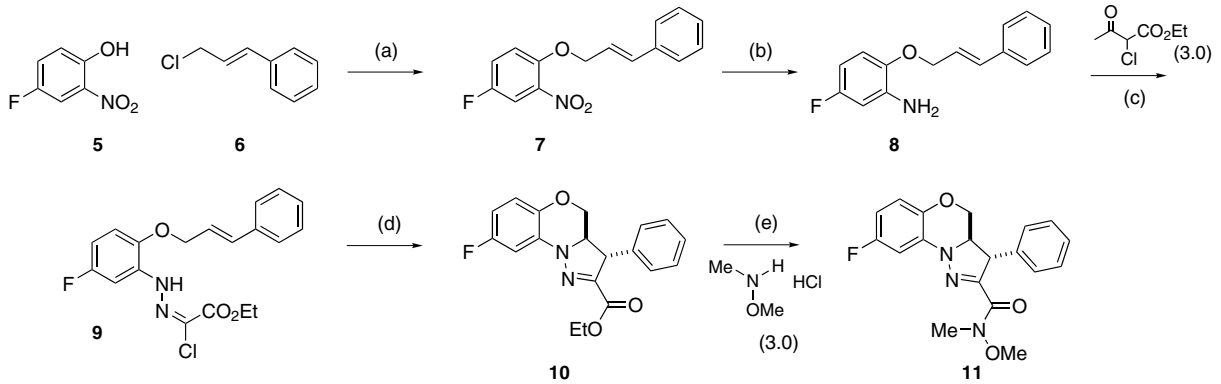

Scheme 1. General synthesis of the pyrazolobenzoxazine (trans-route). Reagents and reaction conditions: (a) K_2CO_3, DMF, 65 °C, 86%; (b) Zn metal, NH_4Cl, MeOH, 55 °C, 89%; (c) $NaNO_2$, HCl/AcOH/H_2O, 65–92%; (d) Et_3N, toluene, 110 °C, 35%; (e) Me_3Al, CH_2Cl_2, 88%.

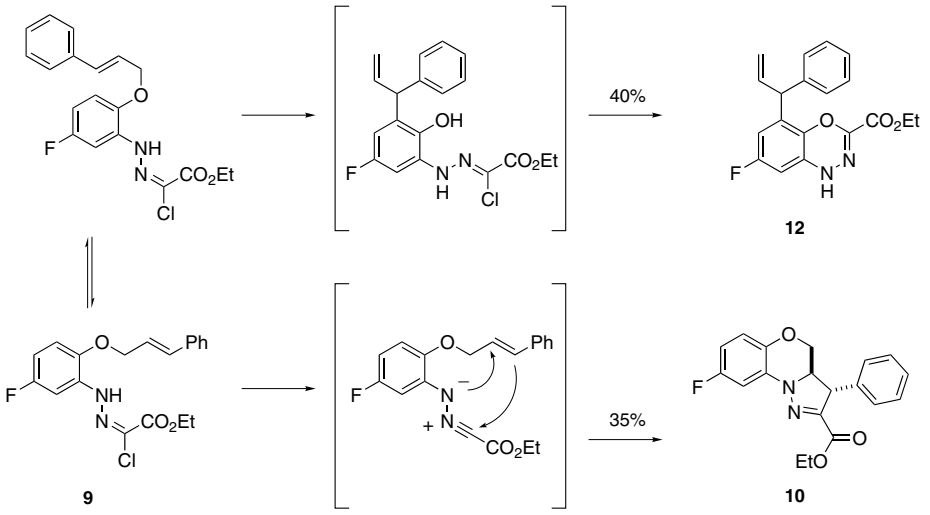

Scheme 2. Preferred side reaction in key [3+2] cycloaddition.

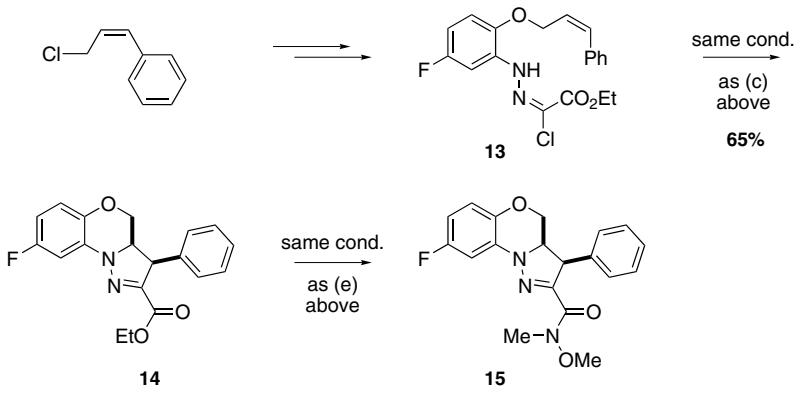

Scheme 3. General synthesis of the pyrazolobenzoxazine (*cis*-route).

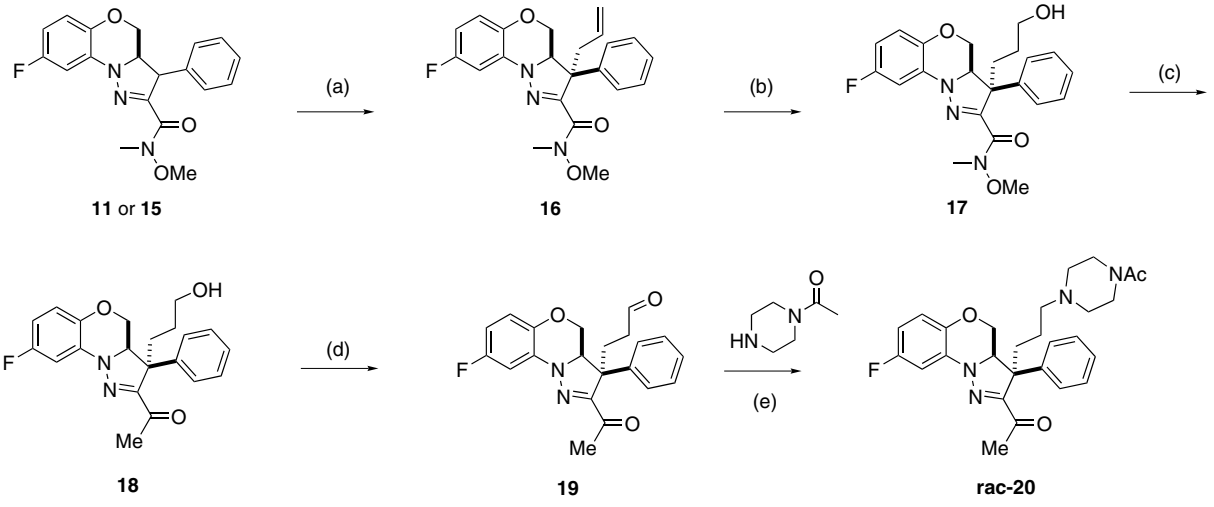

Scheme 4. General synthesis of **20**. Reagents and reaction conditions: (a) LHMDS, allylbromide, 69%, >20:1 de; (b) 9-BBN-H, H_2O_2, THF, 50 °C, 75%; (c) MeLi, THF, 0 °C, 72%; (d) Dess–Martin periodinane, CH_2Cl_2; (e) $Na(OAc)_3BH$, DCE, Et_3N, 80% two step yield.

Dess–Martin periodinane followed by reductive amination with *N*-acetyl piperazine gave the racemic final product **20** in 80% overall yield for the two steps. The final dihydropyrazolobenzoxazine **20** was resolved into its constituent enantiomers using a Chiracel OD column (5 cm column, 100% MeOH, 1 g/injection, RT = 11.6

and 15.5 min, respectively) with the first peak to elute containing the potent enantiomer. Importantly, **20** was found to have aqueous solubility in excess of 4 mg/mL at pH 4 and its absolute stereochemistry was assigned based on prior work, and subsequently confirmed by a X-ray crystallographic structure bound to KSP.[8]

A targeted set of analogs was synthesized by this method taking advantage of the SAR described in earlier efforts. The composite data presented in Table 1 include potency against the KSP enzyme,[9] mitotic arrest activity (Cell EC_{50}) in A2780 human ovarian carcinoma cells,[10] hERG binding,[11] and an MDR ratio. The MDR ratio is expressed as the ratio of cell potency between paired cell lines that have high and low expression of PGP, respectively, and these data have been used extensively in this program as a surrogate measure of Pgp susceptibility.[12] A compound with an MDR ratio < 10 is desirable in our view, and a value of ~1 is ideal.[2]

Consistent with earlier SAR in related series, substitution at R^1 with F, Cl or Me resulted in similar potency and MDR ratios (compounds **20**–**27**). In addition, potency was not greatly altered by the identity of the R^2 amine tethered by the propyl chain at C4. However, substitution at R^2 had significant impact on hERG binding and the MDR ratio, and was thus used to optimize these properties. With respect to hERG binding, amines with reduced basicity (**20**, **24**–**27**, **30**, and **31**) generally showed weaker binding, whereas strongly basic amines (**21**–**23**, **28**, and **29**) engendered a stronger interaction with this ion channel. Similar trends were seen for the MDR ratio, wherein amines with reduced basicity, and tertiary amines tended to have improved potency against the Pgp-overexpressing cell line, and thus lower 'MDR ratios'. Some direct comparisons are worth noting; the comparison of **21** to **28** and **20** to **29** illustrated that capping of the amines resulted in a dramatic reduction in the MDR ratio. These results are in line with the observation that modulating the pK_a of this basic nitrogen or its substitution can balance Pgp-efflux potential with maintenance of KSP potency.

Representative pharmacokinetic data from dog are provided for several compounds in Table 2. In general, these pyrazolobenzoxazines were found to have moderate to high clearance in dog using a cassette dosing strategy. Given its favorable balance of properties (potency, MDR ratio, hERG, and PK), compound **20** was selected for further study.

In the design of these novel KSP inhibitors, efforts have been made to minimize binding to hERG with the hope of avoiding acute cardiotoxicity that would be dose-limiting. While hERG binding is an imperfect predictor for in vivo QT prolongation, it is one of the few available

Table 1. Potency, MDR ratio, and hERG binding

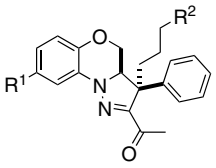

Compound	R^1	R^2	KSP IC_{50}[a] (nM)	Cell EC_{50}[a,b] (nM)	MDR[a] ratio	hERG IC_{50}[a] (nM)
21[c]	F		1.6	7.4	2.3	5940
22[c]	Cl	—NMe$_2$	1.0	4.8	2.5	2000
23[c]	Me		1.8	6.4	2.3	2400
24	F		0.4	4.4	0.8	6100
25[c]	Cl	—N O	1.8	13	1.5	3300
26	Me		1.0	11	1.4	6300
20	F	—N NAc	1.6	5.0	1.0	10,000
27	Cl		1.0	9.0	1.6	5600
28	F	—NH$_2$	0.5	2.5	1.7	940
18	F	—OH	5.2	11	0.6	18,000
29	F	—N NH	4.3	5	40	4600
30	F	—N O NH	1.5	6.9	3.3	17,000
31	F	—N O NMe	0.9	4.8	2.6	9600

[a] See Refs. [9–12] for the details of these assays; all compounds tested as single enantiomers unless noted.
[b] EC_{50} for mitotic arrest (G2/M block) in A2780 cell line.
[c] Tested as a racemate; All values are reported for $n = 3$ or greater with a standard deviation within 25–50% of the reported value.

Table 2. Dog cassette data

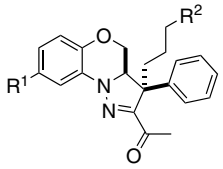

Compound	R^1	R^2	KSP IC_{50}[a] (nM)	Dog pharmacokinetics[a]	
				$t_{1/2}$ (h)	CL (mL/min/kg)
21[b]	F	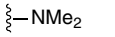	1.6	5.7	52
23[b]	Me		1.8	8.3	37
20	F	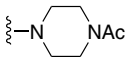	1.6	5.6	14
29	F	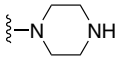	5.2	3.5	40
30	F	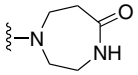	1.5	2.4	15
31	F	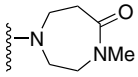	0.9	3.9	11

[a] Dosed iv as a cassette DMSO solution. Average of two dogs dosed at each of 0.25 mg/kg iv. The individual determinations are within ±25% of the mean.
[b] Tested as a racemate.

Table 3. Summarized data for **20**

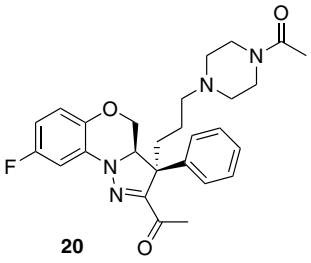

20

Property	**20**
KSP IC_{50} (nM)	1.6
Cell EC_{50} (nM)	5.0
Solubility (pH 4, mg/mL)	>4
MDR ratio	1.0
In vivo mitotic arrest EC_{90} (nM)	100

high throughput assay techniques.[11] Interestingly, we noted that structurally similar compound **1** was found to induce a QTc prolongation in a canine cardiovascular model that was not predicted by hERG binding (>30,000 nM), but corroborated only by measurement of IKr current blockade in a classical patch-clamp assay. Importantly, while **20** demonstrated measurable affinity to hERG (10,000 nM), it did not produce functional blockade in the same patch-clamp study.[13]

As a critical follow-up to these measurements, compound **20** was evaluated for its ability to prolong QTc in vivo in anesthetized dogs. Compound **20** showed no effect on QTc interval when dosed up to 35 μM plasma levels.

Compound **20** was evaluated in our in vivo mouse xenograft tumor model of mitotic arrest.[14] In this pharmacodynamic model, an aqueous solution of **20** was administered to nude mice bearing A2780 xenograft implants via Alzet osmotic pumps for 24 h. The sectioned tumors were stained for phospho-histone H3, an inducible marker of mitotic arrest. KSPi **20** was found to induce maximal mitotic block with a plasma exposure of 100 nM. Based on the similar free fraction of **20** in mouse plasma (3%) and human plasma (3%), this plasma concentration may also produce a similar level of pharmacodynamic potency in human. Intra-tumor levels of compound **20** were not measured in this experiment.

Through the combination of known SAR in two structurally related series, dihydropyrazolobenzoxazines were proposed, synthesized, and found to be highly potent, water-soluble inhibitors of KSP that retained full potency against a Pgp-overexpressing cell line. By utilizing existing SAR and discovering a robust synthetic route highlighted by a diastereoselective installation of a quaternary center, compound **20** was identified as having appropriate potency and pharmacokinetics to further characterize. In a key finding, **20** was shown to have diminished functional interaction with the hERG channel as recorded in a patch-clamp assay relative to another optimized compound (**1**) despite demonstrating tighter binding to the channel. These data prompted examination of **20** in the cardiovascular dog model and were found not to cause QTc prolongation at a plasma concentration 350-fold above the concentration that produced a maximal in vivo pharmacodynamic endpoint in a mouse xenograft model. Based on these

properties, **20** represents a highly optimized lead with ideal properties for a cancer drug (Table 3).[15] In the next letter, efforts to explore a potent structurally related series of KSP inhibitors are described.

Acknowledgments

We thank Dr. Chuck Ross for high resolution mass spectral analysis, Dr. Sandor Varga for NMR identification of **12**, and Mr. Carl Homnick for chiral separations.

Supplementary data

Full experimental details for the synthesis of **20** are provided as an attachment to this manuscript. Supplementary data associated with this article can be found, in the online version, at doi:10.1016/j.bmcl.2007.07.067.

References and notes

1. Preceding communication.
2. Cox, C. D.; Breslin, M. J.; Whitman, D. B.; Coleman, P. J.; Garbaccio, R. M.; Fraley, M. E.; Zrada, M. M.; Buser, C. A.; Walsh, E. S.; Hamilton, K.; Lobell, R. B.; Tao, W.; Abrams, M. T.; South, V. J.; Huber, H. E.; Kohl, N. E.; Hartman, G. D. *Bioorg. Med. Chem. Lett.* **2007**, *17*, 2697.
3. All compounds were characterized by ^{1}H NMR and high resolution mass spectrometry. For detailed experimental procedures, see the supplementary material.
4. Garanti, L.; Sala, A.; Zecchi, G. *J. Org. Chem.* **1977**, *42*, 1389, The undesired Claisen-rearrangement was also observed in this report as a side product.
5. Synthesized in two steps from 3-phenyl-2-propyn-1-ol. Lindlar reduction of the alkyne provided the *cis*-olefin. Conversion of the alcohol to the chloride was accomplished using methanesulfonylchloride, 2,6-lutidine, and LiCl.
6. Levitt, J. I.; Turos, E.; Weinreb, S. M. *Synth. Commun.* **1982**, *12*, 989.
7. Sibi, M. P.; Sharma, R.; Paulson, K. L. *Tetrahedron Lett.* **1992**, *33*, 1941.
8. PDB coordinates for **20**: 2Q2Y.
9. KSP inhibitory activity was measured using a standard ATPase assay. IC_{50} values are reported as averages of at least two determinations; standard deviations are ±25–50%.
10. Mitotic arrest was measured by assessing the mitosis-specific phosphorylation of nucleolin using an antibody coated, bead-based assay. In this assay, total nucleolin is captured on a streptavidin-coated paramagnetic bead coupled with biotinylated nucleolin monoclonal IgG1 antibody 4E2 (Research Diagnostics, Inc.). Nucleolin phosphorylation is detected by an antibody complex consisting of a phospho-specific nucleolin IgM monoclonal antibody, TG3 (Applied NeuroSolutions, Inc.) and a goat anti-mouse IgM labeled with a ruthenium Tris–bipyridyl complex (BV-TAG Technology, BioVeris Corp.). The complex is quantitated via electrochemiluminescence based on the excitation/emission properties of the Tris–bipyridyl complex using a BioVeris M-series analyzer. EC_{50} for KSP-induced nucleolin phosphorylation was determined after treatment with a compound in a 7-point, half-log dilution series for 16 h. The values of EC_{50} are reported as the average of at least two independent determinations; standard deviations are within ±25–50% of EC_{50} values.
11. The hERG IC_{50} values are reported as the average of at least two independent determinations and were acquired by radioligand binding competition experiments using membrane preparations from human embryonic kidney cells that stably express hERG; standard deviations are within ±25–50% of reported values. For assay details, see: Bilodeau, M. T. et al. *J. Med. Chem.* **2004**, *47*, 6363, and references therein.
12. Relative to the parental KB-3-1 cells, KB-V-1 cells, originally derived by culturing KB-3-1 cells in the presence of the Pgp substrate vinblastine (*J. Biol. Chem*. **1986**, *261*, 7762), express >500-fold higher levels of Pgp mRNA and protein. The compound potency (IC_{50}) for induction of mitotic arrest was determined by evaluating the levels of the mitotic marker phospho-nucleolin after 16 h incubation with the test compound in an 11-point half-log dilution series. The ratio of IC_{50} obtained in KB-V-1 cells vs. that in KB-3-1 cells is defined as the MDR ratio. As a general guideline, we considered compounds with MDR ratios < 10 to be of interest for their ability to enter and kill cells that overexpress Pgp. Verapamil, a competitive inhibitor of Pgp, restores the activity of Taxol and our KSP inhibitors in the KB-V-1 cell line to nearly that observed in the parental KB-3-1 line, confirming that Pgp-efflux is responsible for the observed resistance to drug-mediated mitotic arrest. The absolute values of potency between the A2780 and KB cell lines were similar (within 2× of each other).
13. Wang, J.; Della Penna, K.; Wang, H.; Karczewski, J.; Connolly, T. M.; Koblan, K. S.; Bennett, P. B.; Salata, J. J. *Am. J. Physiol.* **2003**, *284*, H256.
14. Athymic nude mice (nu/nu) were xenografted subcutaneously with the human ovarian carcinoma cell line A2780 and the resulting tumors were allowed to reach 200–300 mm^3 before mice were surgically implanted with Alzet mini-pumps (Durect Corporation) filled with the appropriate KSP inhibitors according to manufacturer's recommendations. Prior to the implant, pumps containing KSP inhibitors were primed by incubation in 37 °C water bath for 3 h, so that the pumps would discharge KSP inhibitors at a constant rate of 8 μl/h after subcutaneous implantation. Mice were euthanized 22 h post pump implant and blood and tumors were harvested. Blood was collected in EDTA Vacutainers and processed for plasma to determine pharmacokinetics. Tumors were fixed in 10% neutral buffered formalin and then processed and embedded in paraffin. Paraffin embedded tumors were sectioned 5 μm thick and used in a phospho-histone H3 immunohistochemistry assay designed to determine the percentage of cells blocked in mitosis compared to control treated tumors. After paraffin removal, re-hydration, and antigen retrieval, sections were incubated with anti-phospho-histone H3 (ser10; Upstate). Following incubation with a biotinylated secondary antibody, staining of antigen positive nuclei was accomplished using avidin:biotin complexed horseradish peroxidase and diaminobenzidine reagent. Sections were imaged using an Olympus BX51 microscope with a motorized stage and Image-Pro Analysis software. Quantization of the sections was accomplished by measuring the percentage of positively stained nuclei (black) per unit area.
15. Compound **20** and its analogs are also described in WO2006023083.